

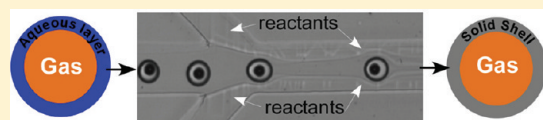
# Coated Gas Bubbles for the Continuous Synthesis of Hollow Inorganic Particles

Jiandi Wan<sup>\*,†</sup> and Howard A. Stone

Department of Mechanical and Aerospace Engineering, Princeton University, Princeton, New Jersey 08544, United States

**S** Supporting Information

**ABSTRACT:** We present a microfluidic approach for the controlled encapsulation of individual gas bubbles in micrometer-diameter aqueous droplets with high gas volume fractions and demonstrate this approach to making a liquid shell, which serves as a template for the synthesis of hollow inorganic particles. In particular, we find that an increase in the viscosity of the aqueous phase facilitates the encapsulation of individual gas bubbles in an aqueous droplet and allows control of the thickness of a thin aqueous shell. Furthermore, because such droplets contain a finite amount of water, uncontrolled hydrolysis reactions between reactive inorganic precursors and bulk water can be avoided. We demonstrate this approach by introducing reactive inorganic precursors, such as silane and titanium butoxide, for sol–gel reactions downstream from the formation of the bubble in a droplet and consequently fabricate hollow particles of silica or titania in one continuous flow process. These approaches provide a route to controlling double-emulsion-type gas–liquid microstructures and offer a new fabrication method for thin-shell-covered microbubbles and hollow microparticles.



Bubbles find a wide range of applications in wastewater treatment,<sup>1</sup> aerated food products,<sup>2</sup> pharmaceuticals, and other biomedical materials such as microbubble-based ultrasound contrast agents.<sup>3</sup> Also, bubbles are used as templates for the synthesis of hollow particles,<sup>4</sup> which are of great interest as catalyst supports, energy storage materials, and drug delivery carriers.<sup>5–8</sup> For example, gas bubbles have been used to assemble nanoparticles on the bubble surface to form shells and consequently produce hollow semiconductor or organometallic particles.<sup>9–11</sup> The majority of the work, however, uses in-situ-generated gas bubbles and therefore requires specific chemical reactions and sometimes involves harmful chemicals. However, gas bubbles generated during acoustic cavitation (ultrasound) can also be used as templates for the synthesis of hollow particles.<sup>12,13</sup> The ultrasound-assisted method is conducted by applying ultrasound to a solution containing surfactants, polymers, and reactive precursors. Subsequently, cavitation microbubbles are generated in the solution and hollow particles are produced by reactions occurring at the gas–liquid interface. The ultrasonic approach provides an effective way to synthesize hollow particles, but it has less control over the shell thickness, the size, and the size distribution of the particles, which, however, are important parameters in many applications.<sup>6,8,14</sup>

Microfluidic devices provide advantages for generating bubbles, foams, and emulsion droplets with narrow size distributions and controlled structures.<sup>15–19</sup> For example, the encapsulation of microbubbles with an organic layer,<sup>20</sup> biopolymers,<sup>21</sup> and the foam-based fabrication of scaffolds for tissue engineering<sup>22</sup> have been achieved via microfluidic approaches. In addition, microfluidic emulsions have been used for the synthesis of hollow particles made from polymer,<sup>23–26</sup> silica,<sup>27,28</sup> carbon,<sup>29</sup> and titania.<sup>30</sup> For the synthesis of sol–gel-based inorganic particles,

these approaches first generate monodisperse droplets and then take advantage of interfacial sol–gel reactions between the droplets and a surrounding immiscible fluid to obtain hollow particles.<sup>27</sup> Although this droplet-based synthesis can provide hollow particles with narrow size distributions, it still lacks the ability to control the shell thickness<sup>28</sup> and requires extra steps (e.g., solvent evaporation) to remove the liquid core.<sup>17</sup> Furthermore, because most of the inorganic precursors are highly reactive with water, specific solvents such as ionic liquids<sup>31</sup> and organic solvents (e.g., formamide<sup>32</sup>) are required to limit the water content for the synthesis of inorganic particles via a sol–gel reaction. Therefore, it remains to develop a simpler, controllable route to synthesize hollow inorganic particles beginning with gas bubbles.

Here we introduce a microfluidic approach where hollow inorganic particles can be generated continuously via sol–gel reactions by using droplets encapsulated with individual gas bubbles as templates. We refer to the continuous formation of droplets containing bubbles as a microbubble emulsion. The fabrication process involves (1) the generation of a monodisperse suspension of aqueous droplets, which encapsulates single gas bubbles at a high gas volume fraction in a continuous oil phase and (2) sol–gel reactions between the aqueous droplets and reactive precursors, which are introduced into the continuous phase via side channels on the same microfluidic device.

This microbubble emulsion-based approach to the synthesis of hollow particles has three advantages: (1) The thickness of the aqueous layer that encapsulates single gas bubbles can be controlled by the flow rates of the individual phases, which could

**Received:** September 29, 2011

**Revised:** November 30, 2011

**Published:** November 30, 2011

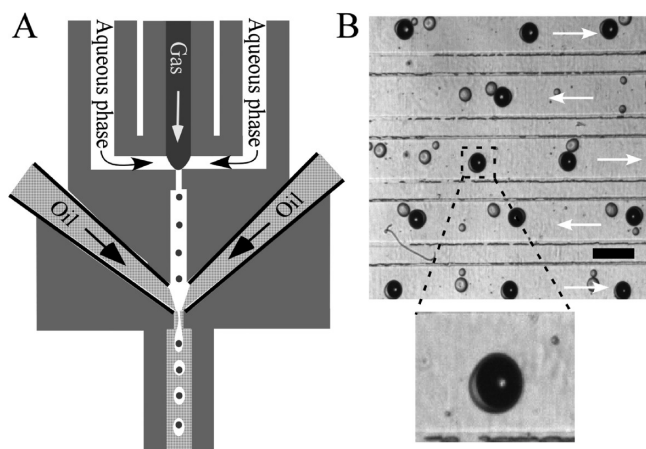


**Figure 1.** Generation of microbubble emulsions. (A) Schematic illustration of the microfluidic setup used to generate the microbubble emulsion. (B) Image of the obtained microbubble emulsion inside a microfluidic channel. The lower image shows an aqueous droplet encapsulating a single gas bubble. Dark spheres are nitrogen gas bubbles. White arrows indicate the flow direction. Note that small droplets (gray spheres) without gas bubbles were produced during the generation of the microbubble emulsions. The continuous oil phase is 50 cSt PDMS with 2 wt % 749 surfactant; the aqueous phase is 90% (v/v) glycerol in deionized water with 2 wt % SDS. The scale bar is 200  $\mu\text{m}$ .

be used as an approach to obtain hollow particles with different shell thicknesses. We provide one example in this letter and demonstrate that the thickness of a silica shell is approximately the same as the thickness of the aqueous layer. (2) A thin aqueous shell makes available only a small volume of water for the sol–gel reaction and hence prevents uncontrolled hydrolysis that is common when excess water is present. (3) Hollow particles are formed in situ and no additional postsynthesis processing is required.

A microbubble emulsion was generated using a double flow-focusing microfluidic design, as we reported previously.<sup>18</sup> Briefly, gas bubbles were generated in a continuous aqueous phase at the first flow-focusing junction and then encapsulated into aqueous droplets that were formed in a continuous oil phase at the second flow-focusing junction (Figure 1A). By changing the oil to aqueous flow rate ratio and the gas pressure, the size of the droplets and bubbles and the number of encapsulated bubbles can be varied systematically.

Single microbubbles encapsulated in a thin aqueous layer, however, are difficult to generate reproducibly.<sup>19</sup> Here, we show that by adding glycerol to the aqueous phase to increase the viscosity, droplets with thin aqueous shells encapsulating single microbubbles can be produced continuously inside the channel (Figure 1B). Further experiments using different concentrations of glycerol in water as the aqueous phase and different viscosities of PDMS as the oil phase confirm that the larger the concentration of glycerol, the thinner the shell of the aqueous droplets (Figure 2).

We use the diameter ratio of the encapsulated gas bubbles to droplets (i.e.,  $D_{\text{bubble}}/D_{\text{droplet}}$ ) to characterize the thickness of the aqueous layer; the larger the  $D_{\text{bubble}}/D_{\text{droplet}}$  value, the thinner the aqueous shell. In particular, when 50 cSt PDMS oil and 90% (v/v) glycerol in water are used as the oil and aqueous phases, respectively, there is a wide range of oil to water flow rate

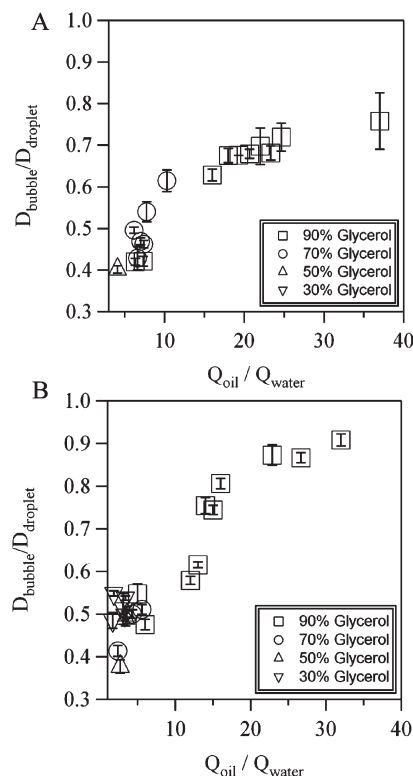


**Figure 2.** Dependence of the bubble diameter to droplet diameter ratio ( $D_{\text{bubble}}/D_{\text{droplet}}$ ) on the normalized flow rate when the continuous phase is (A) 10 and (B) 50 cSt PDMS oil. The continuous oil phase contains 2 wt % 749 surfactant, and the aqueous phase (DI water with various volume percentages of glycerol) contains 2 wt % SDS.

ratios that can be applied to continuously generate aqueous droplets encapsulated with single bubbles with  $D_{\text{bubble}}/D_{\text{droplet}} > 0.5$ . The experimental results show that  $D_{\text{bubble}}/D_{\text{droplet}}$  results as large as 0.9 can be obtained (Figure 2B). The ability to control the thickness of the aqueous shell allows us to use these coated bubbles for the chemical synthesis of the shell.

To demonstrate the application of the microbubble emulsion to the synthesis of inorganic hollow particles, we fabricated a microfluidic device downstream from the double flow-focusing arrangement that had two extra side channels to introduce reactive precursors into the continuous phase, as shown in Figure 3A. Inorganic precursors (e.g., 3,3,3-trifluoropropyl-trichlorosilane (TFP-TCS) or titanium butoxide (TBT)) dissolved at an appropriate concentration in PDMS oil can be added through these side channels. Dissolved precursors diffuse through the oil phase, hydrolyze, and condense at the aqueous layer of the microbubble emulsion to form a solid shell. For example, when 20% (v/v) TFP-TCS in PDMS oil (50 cSt) was introduced into these side channels (Figure 3A), microbubbles with thin silica shells were obtained in situ. Figure 3B and Figure S1 show microscope images of particles collected outside the device. In the microfluidic device, the whole process takes place within tens of seconds and a shell with a thickness of  $4.2 \pm 2 \mu\text{m}$  can be observed around the bubble. Because the uniformity of the thickness of the shell is determined by the position of the bubble encapsulated in the aqueous droplets, which unfortunately changes when droplets flow in the microfluidic channel, the shells are generated with a relatively large deviation in thickness ( $4.2 \pm 2 \mu\text{m}$ ). The thickness of the silica shell, however, is only

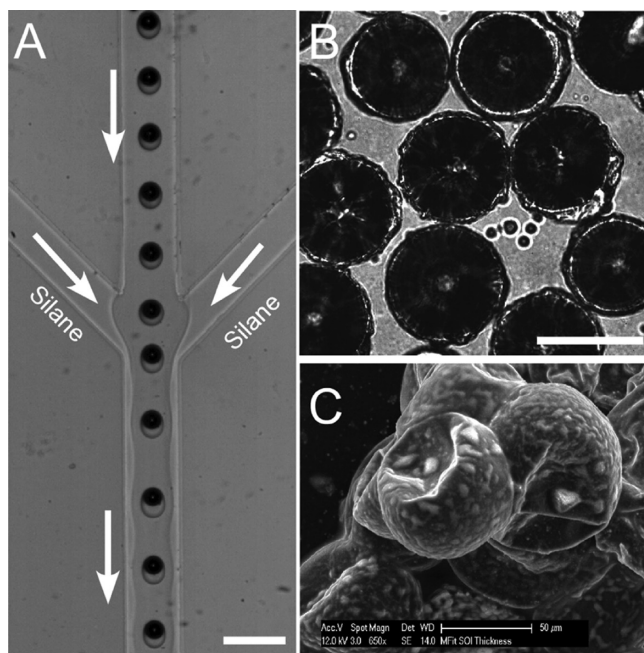


**Figure 3.** On-chip generation of hollow silica particles using 3,3,3-trifluoropropyl-trichlorosilane (TFP-TCS) as a precursor. (A) Image of the microfluidic reactor where TFP-TCS dissolved in PDMS oil (50 cSt) is introduced from the side channels. Aqueous droplets encapsulated with gas bubbles (dark spheres) flow in a continuous PDMS oil phase in the central channel. White arrows indicate the flow direction.  $Q_{oil}/Q_{water} = 10$ . The inlet gas pressure is 27 psi, and the scale bar is 200  $\mu\text{m}$ . (B) Image of hollow silica particles collected outside the microfluidic reactor. The scale bar is 60  $\mu\text{m}$ . (C) SEM image of hollow silica particles. The hollow particles collapse under vacuum inside the SEM sample chamber. The white spots on the shell surface are evidence of some phase separation (Figure S3).

slightly larger than the thickness of the aqueous layer ( $2.8 \pm 0.4 \mu\text{m}$ ) shown in Figure 3A, which demonstrates the ability to control the final shell thickness.

Further characterization by scanning electron microscopy (SEM) of the obtained hollow particles shows that the shell wrinkles or partially collapses but does not break upon exposure to the applied vacuum inside the SEM chamber (Figure 3C and Figure S2). This response suggests that the shell is not brittle. Because there are surfactants in the aqueous and oil phases, we believe that the shell is a mixed composition of surfactants, glycerol, and silica, which may contribute to the observed mechanical features of the shell. Using SEM, we also observed white spots and small particles ( $\sim 200\text{--}600 \text{ nm}$ ) at the shell surface (Figure 3C and Figure S3). Presumably, the small particles with diameters of a few hundred nanometers are crystal particles of TFP-TCS,<sup>28</sup> and their aggregation results in the white spots on the shell surface.

Using the same microfluidic design, we further synthesized hollow titania microparticles using titanium butoxide (TBT) as a reactive precursor in the continuous phase. The hydrolysis of TBT, however, destroyed the microbubble emulsion. Most microbubbles escaped from the encapsulating droplets after TBT was introduced. Surprisingly, however, when a relatively thick aqueous layer of the microbubble emulsion was generated by decreasing the oil to water flow rate ratio (Figure 2B), the obtained microbubble emulsion broke up into small droplets

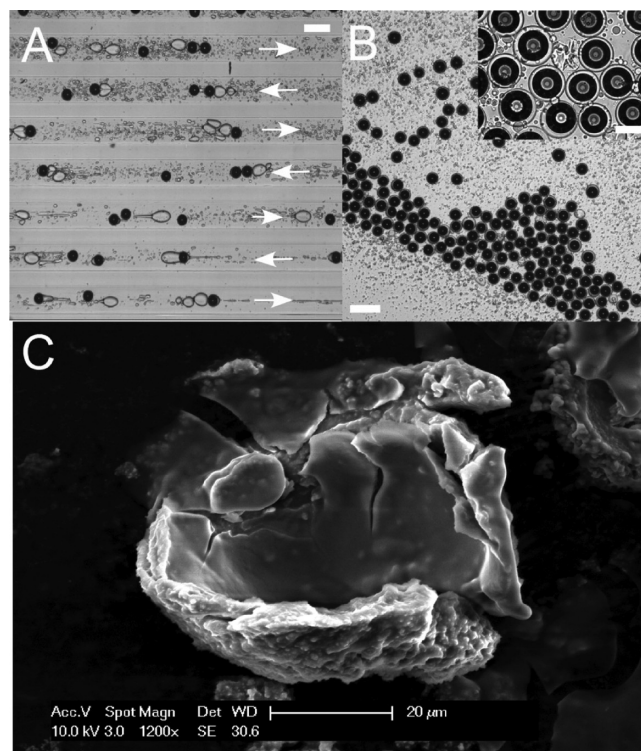


**Figure 4.** On-chip generation of hollow titania particles using titanium butoxide (TBT) as a reactive precursor in the continuous phase. (A) Image of the microbubble emulsion after TBT was introduced. The flow starts from the lower left and leaves at the upper right of the channel. (White arrows indicate the flow direction.) Note that the hydrolysis reaction of TBT destabilizes the emulsion and generates small droplets; there are fewer small particles in the lower section of the channel where the hydrolysis reaction starts, but more particles are generated along the flow direction as the reaction progresses. Dark spheres are gas bubbles. Small drops (particles) are gray in the image.  $Q_{oil}/Q_{water} = 5$ . The inlet gas pressure is 21 psi, and the scale bar is 200  $\mu\text{m}$ . (B) Image of hollow titania particles collected outside the microfluidic reactor. The scale bar is 200  $\mu\text{m}$ . (Inset) High-magnification image of the collected particles. The scale bar is 60  $\mu\text{m}$ . (C) SEM image of hollow titania particles. Two layers, one rough and one smooth, of the shell can be clearly observed.

upon reacting with TBT but left a thin aqueous layer covering the microbubbles intact (Figure 4A). Figure 4B shows the collected particles after they exit the microfluidic channel, where microbubbles covered with a solid shell can be observed. We previously reported a breakup process of the microbubble emulsion at the corners of curved microfluidic channels,<sup>19</sup> and we believe that the breakup process we observe here is a combination of the effects of hydrodynamic flow and chemical reactions.

In contrast to the shells obtained from silica precursors, the shells synthesized from TBT break up under vacuum in the SEM chamber. Further SEM characterization of the obtained hollow titania particles shows that the shell consists of two different layers: a smooth internal layer and a rough outer layer (Figure 4C). The formation of the hierarchical features of the shell appears to be similar to a process described by Steinbacher et al.,<sup>28</sup> where when the aqueous layer is thick the change in the relative rates of hydrolysis and condensation due to the depletion of water determine the shell's morphology. Both in microscopy and the SEM measurements, the thickness of the obtained shell is  $7.9 \pm 2.3 \mu\text{m}$ .

In conclusion, we developed a microbubble emulsion-based continuous flow approach to the synthesis of inorganic hollow particles. We demonstrated that by increasing the viscosity of the aqueous phase, single microbubbles encapsulated with a thin aqueous layer are generated continuously and the thickness of the aqueous layer is controlled by varying the oil to glycerol water flow rate ratio. By introducing downstream silane and metal alkoxides into the flow of the continuous phase, we showed that inorganic hollow particles could be obtained in one step via a sol–gel reaction in the shell covering the bubble. Because the microbubble emulsion produces a finite amount of water in a well-controlled manner, then by our approach uncontrolled hydrolysis reactions in the sol–gel process can be avoided. The microbubble emulsion-based microfluidic approach, therefore, provides an effective strategy for the continuous synthesis of hollow inorganic particles with a controlled shell thickness, which could be used for delivery via routes other than the bloodstream, for example, as depot injections.

## EXPERIMENTAL SECTION

**Experimental Setup.** Microfluidic chips were fabricated in PDMS using standard soft photolithography techniques. Before use, the microfluidic chips were treated with octadecyltrichlorosilane (OTS) to make the glass surface hydrophobic. The water and oil phases are loaded into two syringes (Hamilton) and connected to syringe pumps (Harvard Apparatus, PHD 2000). Pressure is applied to the device that is independently controlled by a regulator (Bellofram, St. Louis, MO) with a precision of 0.1 psi. Polyethylene (PE 20) tubes are connected from the syringe needle to the inlet hole of the channel of the device.

An illustration of the double flow-focusing microfluidic device is shown in Figure 1A. The height of the channels is everywhere equal to 38  $\mu\text{m}$ . The width of the gas-phase and aqueous-phase flow channels is 100  $\mu\text{m}$ ; the width of the central channel where gas bubbles are dispersed in the aqueous phase is 60  $\mu\text{m}$ ; the width of the oil channel is 150  $\mu\text{m}$ ; and the width of the orifices is 20  $\mu\text{m}$ . The width of the two downstream side channels where reactive precursors are introduced is 150  $\mu\text{m}$ , and the width of the central reaction channel is 200  $\mu\text{m}$ . For the flow-rate-dependent measurements, we dispersed pure nitrogen gas bubbles into deionized water with sodium dodecyl sulfate (SDS, 2 wt %, Aldrich) and an appropriate glycerol concentration, after which the aqueous droplets with a single bubble were dispersed in PDMS oil with a given viscosity (10 and 50 cSt PDMS fluid 200). We also add surfactant 749 (2 wt %, Dow Corning) to the oil phase as a surfactant.

**Data Analysis.** Microbubbles and droplets are observed using a high-speed video camera (Phantom V 9, 1400 frames/s) mounted on the microscope. The diameters of the droplets and encapsulated bubbles are analyzed using an image analysis program written in-house with Matlab software. The thickness of obtained inorganic shells is analyzed either by the image analysis program or scanning electron microscopy (FEI, XL30 FEG).

**Sol–Gel Reactions.** For sol–gel reactions, all of the microbubble emulsions were generated by using 90% (v/v) glycerol in deionized water as the aqueous phase and PDMS (50 cSt) as the oil phase. For the synthesis of hollow silica particles, 3,3,3-trifluoropropyl-trichlorosilane (TFP-TCS) (Aldrich) was dissolved in PDMS oil (50 cSt) at 20% (v/v) and then injected into the device through the two downstream side channels, as shown in Figure 3A. Note that a high concentration of TFP-TCS (e.g., 30%) will destroy the emulsion. We note that during the flow process small droplets without internal gas bubbles can also be produced. Because the droplets without internal gas bubbles are small and form solid, high-density particles after the sol–gel reaction, they can be separated by sedimentation or gentle centrifugation.

For the synthesis of hollow titania particles, titanium butoxide (TBT) was dissolved in the PDMS oil phase (50 cSt) at 5% (v/v) and then injected into the device through the two downstream side channels. A high concentration of TBT (e.g., 10%) destroys the emulsion. After the hollow particles were generated, they were collected in a Petri dish outside the device and washed carefully with hexane to remove the oil phase. The particles were then characterized using scanning electron microscopy (FEI, XL30 FEG).

## ASSOCIATED CONTENT

**S Supporting Information.** Microscope and SEM characterizations of hollow silica particles. This material is available free of charge via the Internet at <http://pubs.acs.org>.

## AUTHOR INFORMATION

### Corresponding Author

\*E-mail: [jiandiw@princeton.edu](mailto:jiandiw@princeton.edu).

### Present Addresses

<sup>†</sup>Microsystems Engineering, Rochester Institute of Technology, Rochester, NY 14623.

## ACKNOWLEDGMENT

We thank Princeton University for the financial support of this work.

## REFERENCES

- (1) Albjanic, B.; Ozdemir, O.; Nguyen, A. V.; Bradshaw, D. *Adv. Colloid Interface Sci.* **2010**, *159*, 1–21.
- (2) Zuniga, R. N.; Aguilera, J. M. *Trends Food Sci. Technol.* **2008**, *19*, 176–187.
- (3) Lindner, J. R. *Cardiovasc. Res.* **2009**, *83*, 615–616.
- (4) Lou, X. W.; Archer, L. A.; Yang, Z. *Adv. Mater.* **2008**, *20*, 3987–4019.
- (5) Du, X.; He, J.; Zhao, Y. *J. Phys. Chem. C.* **2009**, *113*, 14151–14158.
- (6) Xu, X.; Asher, S. A. *J. Am. Chem. Soc.* **2004**, *126*, 7940–7945.
- (7) Wu, C.; Xie, Y.; Lei, L.; Hu, S.; OuYang, C. *Adv. Mater.* **2006**, *18*, 1727–1732.
- (8) Ramachandran, S.; Shaheedha, S. M.; Thirumurugan, G.; Dhanaraju, M. D. *Curr. Drug Delivery.* **2010**, *7*, 93–97.
- (9) Hou, H.; Peng, Q.; Zhang, S.; Guo, Q.; Xie, Y. *Eur. J. Inorg. Chem.* **2005**, *13*, 2625–2630.
- (10) Li, X.; Xiong, Y.; Li, Z.; Xie, Y. *Inorg. Chem.* **2006**, *45*, 3493–3495.
- (11) Peng, Q.; Dong, Y.; Li, Y. *Angew. Chem., Int. Ed.* **2003**, *42*, 3027–3030.
- (12) Rana, R. K.; Mastai, Y.; Gedanken, A. *Adv. Mater.* **2002**, *14*, 1414–1418.
- (13) Shchukin, D. G.; Koehler, K.; Moehwald, H.; Sukhorukov, G. B. *Angew. Chem., Int. Ed.* **2005**, *44*, 3310–3314.
- (14) Artemyev, M. V.; Woggon, U.; Wannemacher, R. *Appl. Phys. Lett.* **2001**, *78*, 1032–1034.
- (15) Christopher, G. F.; Anna, S. L. *J. Phys. D* **2007**, *40*, R319–R336.
- (16) Garstecki, P.; Fuerstman, M. J.; Stone, H. A.; Whitesides, G. M. *Lab Chip* **2006**, *6*, 437–446.
- (17) Utada, A. S.; Lorenceau, E.; Link, D. R.; Kaplan, P. D.; Stone, H. A.; Weitz, D. A. *Science* **2005**, *308*, 537–541.
- (18) Wan, J.; Bick, A.; Sullivan, M.; Stone, H. A. *Adv. Mater.* **2008**, *20*, 3314–3318.
- (19) Wan, J.; Stone, H. A. *Soft Matter* **2010**, *6*, 4677–4680.
- (20) Arakawa, T.; Yamamoto, T.; Shoji, S. *Sens. Actuators A* **2008**, *143*, 58–63.

- (21) Park, J. I.; Tumarkin, E.; Kumacheva, E. *Macromol. Rapid Commun.* **2010**, *31*, 222–227.
- (22) Chung, K. Y.; Mishra, N. C.; Wang, C. C.; Lin, F. H.; Lin, K. H. *Biomicrofluidics* **2009**, *3*, 022403.
- (23) Lensen, D.; van Breukelen, K.; Vriezema, D. M.; van Hest, J. C. M. *Macromol. Biosci.* **2010**, *10*, 475–480.
- (24) Liu, L.; Yang, J.-P.; Ju, X.-J.; Xie, R.; Yang, L.; Liang, B.; Chu, L.-Y. *J. Colloid Interface Sci.* **2009**, *336*, 100–106.
- (25) Takeuchi, S.; Garstecki, P.; Weibel, D. B.; Whitesides, G. M. *Adv. Mater.* **2005**, *17*, 1067–1072.
- (26) Zhang, H.; Tumarkin, E.; Peerani, R.; Nie, Z.; Sullan, R. M. A.; Walker, G. C.; Kumacheva, E. *J. Am. Chem. Soc.* **2006**, *128*, 12205–12210.
- (27) Li, D.; Guan, Z.; Zhang, W.; Zhou, X.; Zhang, W. Y.; Zhuang, Z.; Wang, X.; Yang, C. J. *ACS Appl. Mater. Interfaces* **2010**, *2*, 2711–2714.
- (28) Steinbacher, J. L.; Moy, R. W. Y.; Price, K. E.; Cummings, M. A.; Roychowdhury, C.; Buffy, J. J.; Olbricht, W. L.; Haaf, M.; McQuade, D. T. *J. Am. Chem. Soc.* **2006**, *128*, 9442–9447.
- (29) Pan, Y.; Ju, M.; Wang, C.; Zhang, L.; Xu, N. *Chem. Commun.* **2010**, *46*, 3732–3734.
- (30) Eun, T. H.; Kim, S.-H.; Jeong, W.-J.; Jeon, S.-J.; Kim, S.-H.; Yang, S.-M. *Chem. Mater.* **2009**, *21*, 201–203.
- (31) Nakashima, T.; Kimizuka, N. *J. Am. Chem. Soc.* **2003**, *125*, 6386–6387.
- (32) Imhof, A.; Pine, D. J. *Nature* **1997**, *389*, 948–951.